# The Positive Feedback Loop Between RLIP76 and HIF-1α Promotes Glycolysis and Tumorigenesis in Glioma Cells Under Hypoxic Conditions

**Qi Wang**
Shanghai Tongji Hospital
**Chi Zhang**
Shanghai Tongji Hospital
**Lei Zhang**
Shanghai Tongji Hospital
**Huairui Chen**
Shanghai Tongji Hospital
**Jun Qian**
Shanghai Tongji Hospital
**Qingke Bai**
Pudong people's hospital
**Chun Luo** ( luochuntongji@sina.com )
Shanghai Tongji Hospital

**Research**

**Keywords:** Hypoxia, Glycolysis, Glioma, RLIP76, HIF-1α

**Posted Date:** September 24th, 2020

**DOI:** https://doi.org/10.21203/rs.3.rs-76244/v1

# Abstract

Background

Hypoxia is intimately associated with increased glycolysis in gliomas, and HIF-1α plays a critical role in this process. Here, we aim to show that RLIP76 is a novel target of HIF-1α and is involved in hypoxia-enhanced glycolysis in glioma cells.

Methods

The human glioma cell lines U87 and U251 were used to explore the interactions of RLIP76-HIF-1α and RLIP76-VHL using Western blot, a Biotin pull-down assay, Immunoprecipitation, and a Chromatin immunoprecipitation assay under hypoxia. U251 cells pretreated with hypoxia were used for tumor xenografts.

Results

RLIP76 is a novel target of HIF-1α and contributes to hypoxia-enhanced glycolysis in glioma cells. HIF-1α-induced RLIP76 can critically regulate the stability of HIF-1α by alleviating VHL-mediated HIF-1α ubiquitination under hypoxia. RLIP76 interacts with HIF-1α and VHL through an RLIP76 GAP-dependent mechanism. The GAP function of RLIP76 regulates its complex formation because of the dependence of RLIP76 GAP on interactions between RLIP76 and these proteins. RLIP76 knockdown results in decreased U251 cell growth after hypoxia pretreatment in vivo.

Conclusions

This study reveals a positive feedback loop between HIF-1α and RLIP76, suggesting that RLIP76 may undergo a complex series of GAP-dependent interactions with HIF-1α and VHL to protect HIF-1α from degradation while promoting glycolysis under hypoxic conditions. We indicate that RLIP76 is crucial for the regulation of hypoxia-enhanced glycolysis and may provide a new gene therapy approach for glioma patients.


# Background

Glycolysis is a key regulatory pathway for glucose metabolism in aerobic and anaerobic organisms [1]. Glycolysis not only supplies pyruvate to the TCA cycle through oxidative phosphorylation to generate ATP but also helps to produce precursor molecules for protein, nucleic acid and lipid synthesis [2]. Glycolysis is regarded as the main energy source for the rapid proliferation of normal cells. However, enhanced glycolysis and decreased oxidative phosphorylation, known as the Warburg effect, are often observed in various cancerous cells [3]. Emerging evidence suggests that highly proliferating tumor cells can shift their metabolism from mitochondrial glucose oxidation to cytoplasmic glycolysis to meet the energy demands of biosynthesis and bioenergy [4]. In light of this fact, glycolysis inhibition may provide a rational strategy for the long-term management and prevention of cancers.

Hypoxia is a major characteristic of solid tumors, especially in rapidly growing gliomas, which contain incomplete blood vessel networks [5]. Hypoxic conditions induce a molecular response that results in the activation of hypoxia-inducible factor 1α (HIF-1α), a key transcription factor that regulates various genes involved in glioma metabolism and escape from a nutrient-deprived environment [6]. It has been reported that the expression level of HIF-1α increases gradually with increasing pathological grade of glioma, highlighting its importance in glioblastoma (GBM) [7]. In addition, the HIF-1α pathway is a positive regulator of glycolysis, as its suppression can lead to the inhibition of several glycolytic enzymes, which catalyze the irreversible reactions of the glycolytic pathway [8]. Emerging evidence indicates that a high glycolytic rate is the defining characteristic of gliomas and that inhibition of the HIF-1α pathway causes a significant decrease in glycolysis and contributes to the enhancement of oxidative phosphorylation in several glioma cell lines [9–11], reinforcing the important role of HIF-1α in regulating the glycolytic pathway.

RLIP76 is an important member of the GTP enzyme activating protein family [12]. It is thought that RLIP76 participates in the oncogenesis and progression of several cancers by activating a wide array of signaling pathways, such as Ras signaling, which is a key pathway responsible for modulating HIF-1α expression and activity [13–15]. In glioma, RLIP76 is highly expressed and acts as an independent prognostic marker [16]. Several oxygen-dependent chemotherapy drugs (cyclophosphamide, platinum, doxorubicin, etc.) can induce the chemoresistance of various tumor cells by affecting HIF-1α-induced glycolysis [17–20], while RLIP76 knockdown can dramatically enhance the sensitivity of tumor cells to the above chemotherapy drugs [21–23]. Therefore, these results imply that RLIP76 is closely associated with HIF-1α and glycolysis. However, little attention has been paid to the role of RLIP76 in the HIF-1α signaling pathway, and the mechanism of RLIP76-mediated glycolysis is still unclear.

In this study, we identified RLIP76 as an important regulator of glioma progression through suppression of glucose metabolism under hypoxic conditions. Mechanistically, RLIP76 increased the accumulation and stabilization of HIF-1α in a GTPase-activating protein (GAP)-dependent manner by decreasing HIF-1α degradation through von Hippel–Lindau (VHL); in turn, the upregulated HIF-1α could directly interact with RLIP76 in hypoxia to increase glucose consumption and lactate excretion. These results establish RLIP76 as a novel regulator of glucose metabolism that enhances hypoxia-induced glycolysis to facilitate tumor progression.

## Materials And Methods

# Tissue samples and cell culture

The study protocol complied with the National Regulations on the Use of Clinical Samples in China. The use of human specimens in this study was approved by the Specialty Committee on Ethics of Biomedicine Research, Shanghai Tongji University (PJ2015-011-08). Written informed consent was obtained from all participants prior to their participation in the study. The glioma cancer specimens were obtained from patients who underwent surgery at Shanghai Tongji Hospital between July 2016 and July

2018. The malignant glioma cell lines U87 and U251 were obtained from the Chinese Academy of Sciences (Shanghai, China). All glioma cell lines were grown in Dulbecco's Modified Eagle's Medium supplemented with 10% fetal bovine serum (FBS) in a humidified atmosphere containing 5% $CO_2$ at 37 °C.

# Transfection

All processes were performed as previously described [16]. The different synthetic small interfering RNA (siRNA) sequences used are listed in Table S1. The K74M, K425M, R208L, and K224R RLIP76 mutants were constructed as previously described [16]. The full-length human RLIP76 and HIF-1α complementary DNAs (cDNAs), which contained the entire coding sequences, were tagged with GFP (Lenti-RLIP76 and Lenti-HIF-1α) and cloned into the lentiviral vector pLenti6/V5-DEST (Invitrogen).

# Biotin pull-down assay

Biotin pull-down assays were performed as previously described [24]. In vitro-synthesized biotin-labeled RLIP76 (3 mg) was incubated with purified GST, GST-VHL protein, or HIF-1α or VHL deletion mutants for 3 h for the in vitro RNA pull-down assay. The RNA-protein complex was isolated by streptavidin-coupled Dynabeads (Invitrogen).

# Immunoprecipitation assays

Immunoprecipitation was performed using lysates from $1 \times 10^7$ cells treated with RNase A inhibitor and DNase I before centrifugation at 4 °C for 15 min. Cell lysates were incubated with protein A/G beads coated with the indicated antibodies at 4 °C for 3 h and then washed with wash buffer. Total protein was diluted to 1 μg/μl with PBS to decrease the concentrations of detergents. The supernatant was centrifuged and then loaded on 10% SDS-PAGE gels and transferred onto nitrocellulose membranes (Millipore) for Western blot analysis.

# Luciferase assay

U251 cells treated with either control or RLIP76 siRNA were transfected with hypoxia response element (HRE)-WT or HRE-MT reporter plus Renilla luciferase plasmid to investigate the effect of RLIP76 on the activity of the HRE reporter construct. Twelve hours after transfection, cells were cultured under normoxia or hypoxia for another 24 h. A luciferase assay kit (Promega) was used to measure the reporter activity. To explore the effect of HIF-1α on the transcriptional regulation of RLIP76, U251 cells treated with either control or HIF-1α siRNA were cotransfected with a pGL3-based construct containing the RLIP76 promoter plus the Renilla luciferase plasmid. Twenty-four hours after transfection, cells were cultured under normoxia or hypoxia for an additional 24 h. A luciferase assay kit (Promega) was used to measure the reporter activity, which was normalized to Renilla luciferase activity.

# Bioinformatic analysis

LinkedOmics (www.linkedomics.org) helps researchers understand complex correlations among the vast amounts of clinical and molecular attributes of cancers [25]. A LinkedOmics analysis was performed for

The Cancer Genome Atlas (TCGA) GBM database to examine the expression of RLIP76 in GBM. DAVID Bioinformatics Resources 6.8 (http:// david.ncifcrf.gov) was used to perform gene ontology (GO) analysis and Kyoto Encyclopedia of Genes and Genomes (KEGG) analysis on the differentially expressed genes. After analyses were performed to determine the significance and the false discovery rate (FDR), GO terms were selected from the significantly enriched gene sets ($P < 0.05$ and $FDR < 0.05$) as previously described [26]. These analyses were conducted using Gene Set Enrichment Analysis (GSEA) with a minimum number of 5 genes (size), a simulation of 1000 and a P-value of 0.05. PROMO (http://alggen.lsi.upc.es/cgi-bin/promo_v3/promo) is a virtual laboratory for the study of transcription factor binding sites within DNA sequences [27]. We used a PROMO analysis to determine the potential binding sites in the hypoxia response element (HRE) within the RLIP76 promoter region.

# Xenograft analysis

Four-week-old male nude mice were randomly divided into two groups (n = 6 mice per group) and then injected subcutaneously with control or RLIP76 siRNA-transfected U251 cells, which were pretreated with hypoxia for 12 h before injection. Twenty-eight days after injection, the mice were sacrificed, and the tumors were excised and analyzed. Animal studies were approved by the Ethics Committee of the School of Shanghai Tongji Hospital of Tongji University.

# Extracellular acidification rate (ECAR)

The ECAR measurement was performed as previously described [28]. Briefly, the experiment was conducted by an XF96 Extracellular Flux Analyzer (Seahorse Bioscience). Cells were incubated in nonbuffered DMEM containing 10 mM glucose. After the addition of 100 μM oligomycin and 500 mM 2-deoxy-D-glucose, the ECAR was measured under basal conditions.

# Glucose uptake and lactate production

Cellular glucose uptake was evaluated by a fluorescence-based glucose assay kit (BioVision) according to the manufacturer's instructions. To measure lactate production, U87 and U251 cells transfected with either control or RLIP76 siRNA were cultured in normoxia or hypoxia for 24 h. Lactate production was measured using a fluorescence-based lactate assay kit (BioVision).

# Chromatin immunoprecipitation assay (ChIP assay)

U251 cells treated with either control or RLIP76 siRNA were cultured in normoxic or hypoxic conditions for 24 h for ChIP assays. The ChIP assay was conducted according to the protocol of the ChIP assay kit (Upstate Biotechnology, Lake Placid, NY).

# Real-Time RT-PCR

Real-time RT-PCR was performed as previously described [24]. The primers used are listed in Table S1.

# Immunohistochemistry and expression analysis

Immunohistochemistry and expression analysis were performed as previously described [16]. The antibodies used were RLIP76 primary monoclonal antibody (1:500; Abcam, ab56815), HIF-1α monoclonal antibody (1:1000; Abcam, ab51408), and VHL monoclonal antibody (1:500; Abcam, ab238681).

# Western blot analysis

All processes were performed as previously described [16]. The antibodies used were anti-HIF-1 alpha [H1alpha67] (1:500; Abcam, ab1) and VHL monoclonal antibody (1:500; Abcam, ab214778).

# Statistics

All data are expressed as the mean ± SD values from triplicate experiments. Paired groups were compared by Student's t-test, whereas three or more groups were compared by analysis of variance followed by Tukey's test for multiple pairwise comparisons. The correlation between RLIP76 and HIF-1α expression was assessed using Spearman's correlation coefficient. The statistical analysis was performed with SPSS 13.0 software, and $P < 0.05$ was considered statistically significant.

# Results

Hypoxia-Induced RLIP76 is Required for Hypoxia-Enhanced Glycolysis
We first searched for potential hypoxia response elements (HREs) in the RLIP76 promoter to explore whether RLIP76 acts as a hypoxia-responsive gene that participates in hypoxia-enhanced glycolysis in hypoxic conditions. Two potential HREs in the promoter region of RLIP76 were identified by bioinformatics analysis (Figure S1A), which suggests that RLIP76 is a potential hypoxia-responsive gene. Real-time RT-PCR and Western blotting analysis were utilized to explore the expression levels of RLIP76 in U87, U251, SW1088, and A172 glioma cell lines under normoxic or hypoxic conditions. We found that RLIP76 mRNA and protein expression levels were significantly induced by hypoxia in all glioma cells (Figs. 1A and 1B). In addition, RLIP76 was increased under hypoxic conditions in a dose-dependent manner in U251 cells (Figs. 1C and 1D). All these results strongly suggest that RLIP76 is a hypoxia-responsive gene in glioma cells.

To investigate whether RLIP76 is required for the malignant progression of glioma under hypoxic conditions, we exposed U87 and U251 to normoxia or hypoxia (1% O2) for 24 h. As shown in Figure S1B, glioma cells treated with RLIP76 siRNA had a significant decrease in the RLIP76 protein. RLIP76 knockdown suppressed cell proliferation, promoted apoptosis, and inhibited migration, both in normoxic and in hypoxic conditions (Figures S1C-S1E). Moreover, RLIP76 knockdown critically reversed the effect of hypoxia on cell proliferation, apoptosis, and migration (Figures S1C-S1E). These results indicate that RLIP76 critically regulates hypoxia-induced malignant cell progression of gliomas.

We next performed bioinformatics analysis on RLIP76 coexpressed genes to predict the function of RLIP76 in GBM. We investigated 17,084 genes associated with RLIP76 expression by LinkedOmics analysis and displayed them in a heat map (Spearman correlation analysis, $p < 0.05$) that showed genes that are positively (8104 genes) and negatively (8980 genes) correlated with RLIP76 expression in 150

samples from the TCGA GBM database (Figures S2A and S2B). GO analysis and KEGG analysis of RLIP76 coexpressed genes were performed to explore the potential function of RLIP76 in GBM. GO analysis showed that the RLIP76 coexpressed genes were mainly involved in biological processes such as metabolic process, response to stimulus and cell communication. (Figure S2C). KEGG analysis showed that RLIP76 coexpressed genes were mainly involved in signaling pathways such as oxidative phosphorylation and ubiquitin-mediated proteolysis, which are significant processes in the progression of hypoxia-enhanced glycolysis (Figure S2D). These findings prompted us to investigate the relationship between RLIP76 and glucose metabolism. To determine whether RLIP76 modulates glucose metabolism, we explored the effects of RLIP76 knockdown on glucose uptake, lactate production and the extracellular acidification rate (ECAR) in glioma cell lines (U87 and U251) with RLIP76 knockdown by RLIP76 siRNA. Hypoxia treatment resulted in a dramatic enhancement in glucose uptake and lactate production (Figs. 1E and 1F). To confirm these results, we determined the glycolytic capacity by measuring the ECAR, which is mainly caused by the excretion of lactic and carbonic acids during glucose metabolism, in hypoxic U251 cells in hypoxic conditions and revealed substantially enhanced glycolytic capacity (Figs. 1G and 1H). Conversely, all these hypoxia-induced effects were significantly rescued by downregulation of RLIP76 (Figs. 1E–1H), indicating that RLIP76 serves as an important regulator of hypoxia-enhanced glycolysis.

RLIP76 Regulates Hypoxia-Enhanced Glycolysis via a HIF-1α-Dependent Mechanism

Given that the downregulation of RLIP76 significantly inhibited hypoxia-induced glucose metabolism (Figs. 1E–1H), we then investigated LDHA enzymatic activity and the expression of key glycolysis enzymes. RLIP76 knockdown led to a significant suppression of the enhancing effect of hypoxia on LDHA enzymatic activity and LDHA and GLUT1 expression (Figs. 2A–2C). Mounting evidence has revealed that increases in LDHA and GLUT1 induced by hypoxia are regulated by HIF-1α. We next investigated whether RLIP76 regulates hypoxia-enhanced glycolysis by modulating HIF-1α transcriptional activity. Considering that HIF-1α functions by binding to the HRE in hypoxic conditions, we explored the effects of RLIP76 on HIF-1α-regulated luciferase expression using an HRE luciferase reporter system. Hypoxia significantly promoted the luciferase expression of the WT HRE reporter but not the Mut HRE reporter, and this effect was significantly inhibited by downregulation of RLIP76 (Fig. 2D). Furthermore, when HIF-1α activity was suppressed by the HIF-1α inhibitor digoxin or when HIF-1α expression was decreased via HIF-1α-siRNA, the downregulation of RLIP76 had no effects on WT reporter activity under hypoxic conditions (Figs. 2E, 2F, S3A, and S3B). This finding suggests that hypoxia-induced transcription is influenced by RLIP76 through HIF-1α. Notably, we also revealed that the expression levels of hypoxia-induced HIF-1α and HIF-1α target genes (LDHA and GLUT1) were strongly attenuated by RLIP76 inhibition (Fig. 2G), which indicates that RLIP76 plays a significant role in hypoxia-induced HIF-1α signaling pathway. Moreover, overexpression of RLIP76 by Lenti-RLIP76 (an RLIP76 overexpression plasmid) reversed the HIF-1α-mediated reduction in hypoxia induced by RLIP76 knockdown (Figure S3C). These results suggest that RLIP76 modulates HIF-1α transcriptional activity by regulating its expression under hypoxic conditions.

To further explore whether RLIP76 regulates hypoxia-induced glycolysis via HIF-1α, RLIP76 knockdown cells were transfected with exogenous HIF-1α. The effect of RLIP76 inhibition on lactate production (Fig. 2H), ECAR (Fig. 2I), glucose uptake (Fig. 2J), and GLUT1 and LDHA expression (Fig. 2K) was abrogated by exogenous HIF-1α transfection. Together, these results indicate that the acceleration of hypoxia-induced glycolysis caused by RLIP76 is mediated through HIF-1α signaling via the promotion of GLUT1 and LDHA expression.

Hypoxia-Induced RLIP76 Increases HIF-1α Stabilization by Attenuating the VHL-HIF-1α Interaction

We then investigated the mechanism by which hypoxia-induced HIF-1α expression is regulated by RLIP76. Real-time RT-PCR analysis revealed that HIF-1α mRNA levels did not change under hypoxic conditions after RLIP76 knockdown (Fig. 3A). However, RLIP76 inhibition resulted in a significant reduction in the HIF-1α half-life under hypoxic conditions (Fig. 3B). This effect of RLIP76 on HIF-1α was correlated with proteasome-dependent degradation, as the proteasome inhibitor MG132 could restore the RLIP76 knockdown-induced reduction of HIF-1α expression under hypoxic conditions (Fig. 3C). In addition, the RLIP76 knockdown-induced HIF-1α reduction could be reversed by VHL knockdown (Fig. 3D), implying that the effect of RLIP76 on HIF-1α expression is dependent on VHL. The binding of hydroxylated HIF-1α at proline 564 (hyp564) is necessary for VHL-mediated HIF-1α ubiquitination and subsequent degradation. Therefore, we examined the effect of RLIP76 on hyp564-HIF-1α expression levels. RLIP76 knockdown significantly decreased hyp564-HIF-1α expression in hypoxic conditions (Fig. 3B). This effect of RLIP76 on hyp564-HIF-1α could be restored by MG132 treatment (Fig. 3E), indicating that RLIP76 knockdown could promote hyp564-HIF-1α degradation. Moreover, we demonstrated that the stimulatory effect of RLIP76 on hyp564-HIF-1α is depended on VHL without directly influencing HIF-1α hydroxylation status, as VHL inhibition recovered RLIP76 knockdown-caused hyp564-HIF-1α decrease under both normoxic and hypoxic conditions (Fig. 3D), while no significant difference was observed on hyp564-HIF-1α expression in VHL-knockdown cells upon downregulation of RLIP76 under hypoxia (Figure S3D). As predicted, RLIP76 inhibition significantly enhanced HIF-1α polyubiquitination under hypoxia (Fig. 3F). Consistent with these findings, the polyubiquitination of hypoxic HIF-1α was significantly increased in RLIP76-siRNA-transfected cells (RLIP76 knockdown cells) and returned to that of the controls upon restoration of RLIP76 by transfecting the Lenti-RLIP76 plasmid (RLIP76-overexpressing cells) (Fig. 3G). We further demonstrated that RLIP76 knockdown promoted HIF-1α-VHL and hyp465-HIF-1α-VHL associations under hypoxic conditions (Figs. 3H and 3I). As illustrated in Fig. 3J, RLIP76 was able to suppress the associations between VHL and HIF-1α. Collectively, these data imply that hypoxia-induced RLIP76 attenuates the interaction of VHL and HIF-1α to inhibit the VHL-mediated degradation of HIF-1α by the ubiquitin–proteolytic pathway.

It has been shown that RLIP76 can function as a regulator of heat shock factor by interfering with its ability to form complexes with its target molecules [13], and we hypothesized that RLIP76 could attenuate the VHL-HIF-1α interaction in a similar manner. As shown in Fig. 4A and 4B, RLIP76 could bind to VHL and HIF-1α according to immunoprecipitation assays. The complexes formed between RLIP76-HIF-1α and RLIP76-VHL were also confirmed by GST pull-down of endogenous RLIP76 (Figs. 4C, and 4D). A subsequent co-IP assay further demonstrated that RLIP76 was not capable of forming a trimeric complex

with VHL and HIF-1α (Fig. 4E), implying that there is a competitive interaction among RLIP76, HIF-1α and VHL.

To determine the structural factors for RLIP76-VHL and RLIP76-HIF-1α complex formation, we conducted deletion mapping experiments. The mutant VHL (aa 54–213, aa 54–213), which is known to be able to interact with HIF-1α, was found in a complex with RLIP76, while the other three VHL deletion mutants (aa 72–213, 1–156, and 1–186) without HIF-1α-binding ability showed no interaction with RLIP76 (Figs. 4F and 4G), which implies that RLIP76 and HIF-1α might competitively interact with VHL. In addition, all HIF-1α deletion mutants could interact with RLIP76 (Figs. 4H and 4I), which suggests that RLIP76 could be associated with HIF-1α via multiple domains. All these data suggest that RLIP76 may affect the HIF-1α-VHL complex by directly interacting with each protein.

Significance of the GAP Function of RLIP76 in the Interaction with HIF-1α and VHL

The RLIP76 protein serves as an ATP-binding plasma membrane transporter with two ATP-binding sites at residues 69–74 and 418–425 [16]. RLIP76 ATPase activity has been well documented to be involved in the regulation of multiple pathways, including the ubiquitin–proteolytic pathway. Using RLIP76 ATP-binding mutants (K74M and K425M), we then explored whether the ATPase activity of RLIP76 is necessary for its interactions with HIF-1α and VHL. ATPase RLIP76 mutants appeared to form complexes with HIF-1α or VHL (Figs. 4J-4N), which indicates an ATP-independent role for RLIP76 in its interactions with HIF-1α and VHL.

RLIP76 was first cloned as a Ral-binding GTPase-activating protein (GAP) and negative regulator of heat shock factor-1 (Hsf-1) because of its ability to form the RLIP76-Hsf-1 complex, which is due to the GAP function of RLIP76. We then utilized GAP-deficient R208L and K224R RLIP76 mutants to explore the effect of RLIP76 on HIF-1α or VHL complex formation. In contrast to ATP-deficient mutants, the R208L and K244R RLIP76 mutants failed to integrate with HIF-1α or VHL (Figs. 4J-4N), suggesting the involvement of the GAP function of RLIP76 in binding to HIF-1α and VHL. Overall, the GAP function of RLIP76, but not the ATPase function, is required for formation of the RLIP76-HIF-1α and RLIP76-VHL complexes.

RLIP76 is a Novel Transcriptional Target of HIF-1α

To investigate the molecular mechanism of aberrant RLIP76 expression induced by hypoxia, we inhibited HIF-1α, HIF-2α, and p53, known as classical hypoxia-responsible transcriptional factors, in U251 cells. Downregulation of HIF-1α, but not HIF-2α or p53, strongly alleviated RLIP76 mRNA and protein upregulation induced by hypoxia (Figs. 5A and 5B). In addition, overexpression of HIF-1α greatly increased RLIP76 expression in a dose-dependent manner (Fig. 5C). U251 cells treated with $CoCl_2$ or DMOG (known as HIF-1α inducers) showed a significant increase in RLIP76 mRNA expression (Fig. 5D). These findings indicate that HIF-1α is associated with hypoxia-induced RLIP76 expression. We then explored the effect of HIF-1α on the regulation of RLIP76 expression at the transcriptional level. We found two putative HREs in the promoter of the RLIP76 gene by using PROMO analysis (Figure S1A). Subsequent ChIP assays confirmed the interaction of HIF-1α and HRE-containing genomic DNA fragments (P1 and P2) in RLIP76 under hypoxic conditions (Fig. 5E). By constructing a firefly luciferase reporter plasmid containing wild-type (WT) or mutant (Mut) HREs in the promoter region, we further

explored whether the RLIP76 HREs are necessary for HIF-1α-dependent transcriptional activity. As predicted, hypoxia induced dramatically higher luciferase expression in the WT reporter than in the Mut reporter (Figs. 5F and 5G). Moreover, hypoxia-induced luciferase expression was significantly suppressed by HIF-1α inhibition (Figs. 5H and 5I). These results suggest that RLIP76 is a direct transcriptional target of HIF-1α.

Hypoxia-Induced RLIP76 is Critical for the Regulation of Tumorigenesis

To investigate the possible correlation between hypoxia-induced RLIP76 and tumorigenesis in vivo, we established a xenograft glioma model. U251 cells were pretreated with hypoxia to activate the HIF-1α/RLIP76 pathway before injection into the flanks of nude mice. Downregulation of RLIP76 inhibited the tumorigenicity of U251 cells, as demonstrated by the tumor volume results (Figs. 6A and 6B). BrdUrd incorporation revealed that cell proliferation was dramatically suppressed in RLIP76 knockdown tumors compared with control tumors (Fig. 6C). The apoptotic cells in xenograft gliomas were observed by TUNEL staining, and RLIP76 downregulation resulted in a significant increase in RLIP76 knockdown tumors (Fig. 6D). Immunohistochemical (IHC) analysis showed that the expression level of CD31 was significantly decreased in tumors derived from RLIP76 knockdown cells compared with those derived from control transfectants (Fig. 6E). In addition, real-time RT-PCR analysis indicated that the expression levels of HIF-1α, LDHA, and GLUT1 were effectively downregulated, whereas the VHL expression level was dramatically upregulated in RLIP76 knockdown xenografts compared with the control (Fig. 6F). These data strongly indicate that RLIP76 enhances cell proliferation and angiogenesis in vivo and suggest that the hypoxia-induced RLIP76 axis plays a critical role in promoting tumorigenesis. We further investigated RLIP76, HIF-1α, and VHL expression in 96 human GBM samples by IHC staining (Fig. 6G). RLIP76-high GBM exhibited considerably higher immunoreactivity for HIF-1α and lower immunoreactivity for VHL expression (Fig. 6H). Spearman's correlation analysis revealed that RLIP76 expression was positively associated with HIF-1α by immunostaining (Figure S3E). As we expected, a significant reverse association was also found between VHL and RLIP76 expression (Figure S3F). Together, these data demonstrate that hypoxia-induced RLIP76 plays a key role in cellular mechanisms related to glucose metabolism and glioma progression in vivo.

# Discussion

RLIP76 is an ATP-dependent transporter that has been implicated in the transportation of anionic metabolites, such as glutathione conjugates of electrophile compounds [29]. In addition to its function as a transporter, RLIP76 also acts as a regulator of the cell response to oxidant injury [30]. Previous studies have reported that Hsf-1 binds to RLIP76, which is required for the response to oxidative stress [31]. Oxidative stress-induced injury may not only induce apoptosis and autophagy, but it may also affect energy metabolism in the cell [32, 33]. Energy metabolism is primarily manifested as the tricarboxylic acid cycle, the mitochondrial oxidative respiratory chain, inhibition of oxidative phosphorylation and enhancement of glycolysis. Increased glycolysis effectively enhances the energy supply under conditions of hypoxia-induced oxidative stress injury, which is regarded as a typical tumor adaptive response [34,

35]. Here, we identified RLIP76 as a hypoxia-inducible molecule that is necessary for hypoxia-enhanced glycolysis, which suggests that non-ABC transporters might contribute to the Warburg effect.

Enhanced glycolysis and decreased oxidative phosphorylation have been viewed as identical features of aberrant metabolism that maintain the viability of tumor cells in gliomas [36]. Although there is new interest in the energy metabolism of gliomas, it is generally believed that the metabolic defects of tumor cells and the Warburg effect are mainly due to select genomic mutability during tumor development [3]. Here, we performed bioinformatic analysis on RLIP76 coexpressed genes from the TCGA GBM database and found that RLIP76 plays a crucial role in the reduction of oxidative phosphorylation and ubiquitin-mediated proteolysis in GBM. It has been well documented that the ubiquitin- and proteasome-mediated degradation of HIF-1α plays a pivotal role in enhanced glycolysis in GBM [37]. Under hypoxic conditions, HIF-1α can escape ubiquitin-mediated proteolysis by disassociating with VHL, a component of an E3 ubiquitin-protein ligase complex [38]. VHL has been regarded as an important member of the ubiquitin-mediated proteolysis pathway during HIF-1α degradation. In the absence of VHL, HIF-1α accumulates, leading to better adaptation to low-nutrient environments and survival in hypoxia [39]. We found that the level of HIF-1α was greatly reduced after RLIP76 knockdown in a xenograft mouse model, whereas the level of VHL was increased. In addition, a positive association was found between HIF-1α and RLIP76, while a negative correlation was found between VHL and RLIP76 in GBM specimens. These results strongly imply that RLIP76 has a close functional relationship with HIF-1α and VHL in vivo and may facilitate glycolysis by regulating them in GBM.

Hypoxia leads to enhanced expression of HIF-1α, HIF-2α and p53, which are classical oxygen-dependent transcriptional activators [40]. Here, we showed that only HIF-1α downregulation, not HIF-2α or p53 downregulation, significantly suppressed hypoxia-induced RLIP76 overexpression in GBM. These results are consistent with previous studies showing that knockdown of RLIP76 can inhibit tumor progression in different human neoplasms of the central nervous system, such as GBMs and neuroblastomas, independent of p53 status [16, 41]. These studies, together with ours, suggest that RLIP76 may be fundamental to the HIF-1α-induced signaling pathway and that its relationship to tumor cell energy is pivotal. In addition to the interactions between RLIP76-HIF-1α and RLIP76-VHL, several other hypoxia-induced molecules, such as Hsf-1 and HSP90, have recently been shown to form complexes with RLIP76 to control the hypoxia-induced oxidative stress response [42, 43]. Specifically, a GAP-dependent role for RLIP76 in interacting with Hsf-1 has been reported, as RLIP76 promotes Hsf-1 translocation into the nucleus and therefore functions to suppress Hsf-1 by increasing heat shock protein transcription [42]. In the present study, we further reveal the critical genomic structure of RLIP76 in complex formation under hypoxic conditions in which the GAP function but not the ATPase function of RLIP76 is essential for the RLIP76-HIF-1α and RLIP76-VHL interactions in glioma cells. Intriguingly, we previously found that the ATPase function of RLIP76 is required for the degradation of Rac1 by the ubiquitin–proteolytic pathway under normoxic conditions in glioma cells [16]. All these findings confirm that RLIP76 is a multifunctional protein that contributes to gene regulation by catalyzing modifications of various transcription factors to facilitate tumor progression.

The enhancement of glycolysis is a principal characteristic of energy metabolism during glioma development in hypoxic conditions [10]. It has been demonstrated that HIF-1α activation in response to hypoxic stimuli can constitutively promote the expression of glycolytic genes, such as LDHA, GLUT1, HK2 and PKM2, in GBM cells to regulate tumor glycolysis [11, 44]. Here, we demonstrated that RLIP76 drives a positive feedback loop to promote the HIF-1α-related signaling pathway by stabilizing HIF-1α, leading to the promotion of hypoxia-induced glycolysis in hypoxic conditions. It has also been shown that the binding of RLIP76 to VHL has an inhibitory effect on the binding of VHL and HIF-1α, which is necessary for the VHL-induced ubiquitin degradation of HIF-1α. This suppression is attributed to the fact that after competitively binding to VHL, which means that RLIP76-VHL complex formation will further prevent HIF-1α from interacting with VHL, RLIP76 could induce HIF-1α activation and ultimately promote glycolysis. Lee et al. previously found that RLIP76 may regulate the function of HIF-1 in tumor cells without affecting HIF-1 expression [45]. Here, we confirmed that upregulation of RLIP76 is capable of restoring RLIP76 knockdown-induced decrease in HIF-1α under hypoxia, while RLIP76 overexpression failed to enhance HIF-1α expression under normoxia, which is consistent with a previous study. Considering the above results, we believe that the suppressive effect of RLIP76 on the HIF-1α-VHL interaction might be part of the mechanism for RLIP76-induced HIF-1α activation in hypoxia.

The HIF-1α signaling pathway is a positive regulator of cancer proliferation, as its suppression often results in tumor suppression [6, 38]. It has been reported that HIF-1α is aberrantly expressed and inversely associated with prognosis in GBM patients [46]. Moreover, either suppressing HK2 activity by its inhibitor 3-bromopyruvate or downregulating LDHA by siRNA inhibits the malignant phenotype of glioma cells, suggesting that HIF-1α-responsive genes related to glycolysis could be potential targets for glioma treatment [47, 48]. It has been well established that RLIP76 has a close association with several HIF-1α-related genes, such as VEGFA and AKT, which leads to malignant development of gliomas [45, 49]. Here, we reveal that knockdown of hypoxia-induced RLIP76 results in the suppression of U251 cell tumorigenicity by using a xenograft mouse model and demonstrate that RLIP76 may serve as a vital oncogene in GBM by participating in the HIF-1α signaling pathway. These findings suggest that inhibition of RLIP76 may provide a novel and promising method for glioma therapy.

# Conclusions

In conclusion, we describe the interaction of RLIP76, HIF-1α and VHL in the regulation of hypoxia-enhanced glycolysis under hypoxic conditions (Fig. 6I). RLIP76 functions as a hypoxia-responsive gene that is rapidly induced by HIF-1α. Then, RLIP76 promotes the stability of HIF-1α by disrupting the HIF-1α-VHL complex, and by doing so, it leads to increased expression levels of HIF-1α target genes (LDHA and GLUT1) and ultimately enhances glycolysis. Therefore, a better understanding of RLIP76-mediated HIF-1α signaling could contribute to the development of combination therapies and become a potential strategy for GBM treatment in the future.

# Abbreviations

AKT
Protein kinase B
ATP
adenosine triphosphate
ChIP
Chromatin  immunoprecipitation
ECAR
Extracellular acidification rate
FDR
false discovery rate
GAP
GTPase-activating protein
GBM
glioblastoma
GLUT1
Glucose transporter type 1
GO
gene ontology
GSEA
Gene Set Enrichment Analysis
GTP
Guanosine triphosphate
HIF-1α
hypoxia-inducible factor 1α
HRE
hypoxia response element
Hsf-1
heat shock factor-1
KEGG
Kyoto Encyclopedia of Genes and Genomes
LDHA
lactate dehydrogenase A
TCA cycle
tricarboxylic acid cycle
TCGA
The Cancer Genome Atlas
VEGFA
vascular endothelial growth factor A
VHL
von Hippel–Lindau

## Declarations

# Ethics approval and consent to participate

All the patients were informed of sample collection and usage. The tissue samples were collected and used in accordance with approval by the Specialty Committee on Ethics of Biomedicine Research, Shanghai Tongji University (PJ2015-011-08). Use of animal was approved by the Shanghai Tongji hospital animal ethic committee.

### Consent for publication

Not applicable.

### Availability of data and materials

The data that support the findings of this study are available from the corresponding author upon reasonable request.

### Competing interests

The authors declare that they have no competing interests.

# Funding

This study was funded by the National Science Foundation of China (grant no. 81802489), the Shanghai Natural Science Foundation (grant nos. 18ZR1434500, 19ZR1448900 and 18411962500), the Featured Clinical Discipline Project of Shanghai Pudong (grant no. PWYst2018-01) and the Key Discipline Group Construction Project of Shanghai Pudong (grant no. PWZxq2017-02).

# Contributions

CZ and QW were responsible for designing the study and writing the manuscript. LZ and HRC were responsible for data analysis. JQ was responsible for editing the manuscript. QKB and CL were responsible for re-editing the manuscript. All authors read and approved the final manuscript.

# Acknowledgements

Not applicable

## References

1. Li Z, Zhang H. Reprogramming of glucose, fatty acid and amino acid metabolism for cancer progression. Cell Mol Life Sci. 2016;73(2):377–92.
2. Smith RL, et al. Metabolic Flexibility as an Adaptation to Energy Resources and Requirements in Health and Disease. Endocr Rev. 2018;39(4):489–517.
3. Hainaut P, Plymoth A. Cancer as a metabolic disease. Curr Opin Oncol. 2012;24(1):56–7.
4. Poljsak B, et al., *Cancer Etiology: A Metabolic Disease Originating from Life's Major Evolutionary Transition?* Oxid Med Cell Longev, 2019. **2019**: p. 7831952.
5. Karsy M, et al. Correlation of Glioma Proliferation and Hypoxia by Luciferase, Magnetic Resonance, and Positron Emission Tomography Imaging. Methods Mol Biol. 2018;1742:301–20.
6. Kaur B, et al. Hypoxia and the hypoxia-inducible-factor pathway in glioma growth and angiogenesis. Neuro Oncol. 2005;7(2):134–53.
7. Liu Y, et al. The expression and significance of HIF-1alpha and GLUT-3 in glioma. Brain Res. 2009;1304:149–54.
8. Wang Y, et al. Characterization of HIF-1alpha/Glycolysis Hyperactive Cell Population via Small-Molecule-Based Imaging of Mitochondrial Transporter Activity. Adv Sci (Weinh). 2018;5(3):1700392.
9. Wang G, et al. Advances in the targeting of HIF-1alpha and future therapeutic strategies for glioblastoma multiforme (Review). Oncol Rep. 2017;37(2):657–70.
10. Blum R, et al. Ras inhibition in glioblastoma down-regulates hypoxia-inducible factor-1alpha, causing glycolysis shutdown and cell death. Cancer Res. 2005;65(3):999–1006.
11. Zhang L, et al. Clk1-regulated aerobic glycolysis is involved in glioma chemoresistance. J Neurochem. 2017;142(4):574–88.
12. Singhal SS, et al. RLIP76 Inhibition: A Promising Developmental Therapy for Neuroblastoma. Pharm Res. 2017;34(8):1673–82.
13. Mott HR, Owen D. Structure and function of RLIP76 (RalBP1): an intersection point between Ras and Rho signalling. Biochem Soc Trans. 2014;42(1):52–8.
14. Kidd AR 3. Ras-related small GTPases RalA and RalB regulate cellular survival after ionizing radiation. Int J Radiat Oncol Biol Phys. 2010;78(1):205–12. rd, et al, , ( .
15. Zhang X, et al. Interaction between p53 and Ras signaling controls cisplatin resistance via HDAC4- and HIF-1alpha-mediated regulation of apoptosis and autophagy. Theranostics. 2019;9(4):1096–114.
16. Wang Q, et al. RLIP76 is overexpressed in human glioblastomas and is required for proliferation, tumorigenesis and suppression of apoptosis. Carcinogenesis. 2013;34(4):916–26.
17. Xu Y, et al. ABT737 reverses cisplatin resistance by targeting glucose metabolism of human ovarian cancer cells. Int J Oncol. 2018;53(3):1055–68.
18. Wang B, et al., *Systemic chemotherapy promotes HIF-1alpha-mediated glycolysis and IL-17F pathways in cutaneous T-cell lymphoma*. Exp Dermatol, 2020.

19. Ren X, Su C. Sphingosine kinase 1 contributes to doxorubicin resistance and glycolysis in osteosarcoma. Mol Med Rep. 2020;22(3):2183–90.
20. Zhang Y, Liu Y, Xu X. Knockdown of LncRNA-UCA1 suppresses chemoresistance of pediatric AML by inhibiting glycolysis through the microRNA-125a/hexokinase 2 pathway. J Cell Biochem. 2018;119(7):6296–308.
21. Herlevsen MC, Theodorescu D, *Mass spectroscopic phosphoprotein mapping of Ral binding protein 1 (RalBP1/Rip1/RLIP76).* Biochem Biophys Res Commun, 2007. **362**(1): p. 56–62.
22. Nagaprashantha LD, et al. 2'-Hydroxyflavanone effectively targets RLIP76-mediated drug transport and regulates critical signaling networks in breast cancer. Oncotarget. 2018;9(26):18053–68.
23. Leake K, et al. RLIP76 regulates PI3K/Akt signaling and chemo-radiotherapy resistance in pancreatic cancer. PLoS One. 2012;7(4):e34582.
24. Yang F, et al. Reciprocal regulation of HIF-1alpha and lincRNA-p21 modulates the Warburg effect. Mol Cell. 2014;53(1):88–100.
25. Vasaikar SV, et al. LinkedOmics: analyzing multi-omics data within and across 32 cancer types. Nucleic Acids Res. 2018;46(D1):D956–63.
26. Wang Q, et al. Increased RLIP76 expression in IDH1 wildtype glioblastoma multiforme is associated with worse prognosis. Oncol Rep. 2020;43(1):188–200.
27. Messeguer X, et al. PROMO: detection of known transcription regulatory elements using species-tailored searches. Bioinformatics. 2002;18(2):333–4.
28. Feng Y, et al. A20 targets PFKL and glycolysis to inhibit the progression of hepatocellular carcinoma. Cell Death Dis. 2020;11(2):89.
29. Vatsyayan R, et al. RLIP76: a versatile transporter and an emerging target for cancer therapy. Biochem Pharmacol. 2010;79(12):1699–705.
30. Awasthi S, et al. Transport functions and physiological significance of 76 kDa Ral-binding GTPase activating protein (RLIP76). Acta Biochim Pol. 2002;49(4):855–67.
31. Matarrese P, et al. Gender disparity in susceptibility to oxidative stress and apoptosis induced by autoantibodies specific to RLIP76 in vascular cells. Antioxid Redox Signal. 2011;15(11):2825–36.
32. Blasiak J, et al. Oxidative stress, hypoxia, and autophagy in the neovascular processes of age-related macular degeneration. Biomed Res Int. 2014;2014:768026.
33. Lee P, Chandel NS, Simon MC. Cellular adaptation to hypoxia through hypoxia inducible factors and beyond. Nat Rev Mol Cell Biol. 2020;21(5):268–83.
34. Deveci HA, et al. Alpha lipoic acid attenuates hypoxia-induced apoptosis, inflammation and mitochondrial oxidative stress via inhibition of TRPA1 channel in human glioblastoma cell line. Biomed Pharmacother. 2019;111:292–304.
35. Lu J, Tan M, Cai Q. The Warburg effect in tumor progression: mitochondrial oxidative metabolism as an anti-metastasis mechanism. Cancer Lett. 2015;356(2 Pt A):156–64.

36. Poff A, et al. Targeting the Warburg effect for cancer treatment: Ketogenic diets for management of glioma. Semin Cancer Biol. 2019;56:135–48.
37. Gabriely G, et al. Role of AHR and HIF-1alpha in Glioblastoma Metabolism. Trends Endocrinol Metab. 2017;28(6):428–36.
38. Semenza GL. Hypoxia-inducible factor 1 (HIF-1) pathway. Sci STKE. 2007;2007(407):cm8.
39. Maxwell PH, et al. The tumour suppressor protein VHL targets hypoxia-inducible factors for oxygen-dependent proteolysis. Nature. 1999;399(6733):271–5.
40. Fuhrmann DC, et al. Chronic hypoxia alters mitochondrial composition in human macrophages. Biochim Biophys Acta. 2013;1834(12):2750–60.
41. Singhal J, et al. Targeting p53-null neuroblastomas through RLIP76. Cancer Prev Res (Phila). 2011;4(6):879–89.
42. Sahu M, et al. Lens specific RLIP76 transgenic mice show a phenotype similar to microphthalmia. Exp Eye Res. 2014;118:125–34.
43. Awasthi S, et al. Transport of glutathione conjugates and chemotherapeutic drugs by RLIP76 (RALBP1): a novel link between G-protein and tyrosine kinase signaling and drug resistance. Int J Cancer. 2003;106(5):635–46.
44. Maurer GD, et al., *Knockdown of the TP53-Induced Glycolysis and Apoptosis Regulator (TIGAR) Sensitizes Glioma Cells to Hypoxia, Irradiation and Temozolomide*. Int J Mol Sci, 2019. 20(5).
45. Lee S, Goldfinger LE. RLIP76 regulates HIF-1 activity, VEGF expression and secretion in tumor cells, and secretome transactivation of endothelial cells. FASEB J. 2014;28(9):4158–68.
46. Liu Q, Cao P. Clinical and prognostic significance of HIF-1alpha in glioma patients: a meta-analysis. Int J Clin Exp Med. 2015;8(12):22073–83.
47. Xu DQ, et al. 3-Bromopyruvate inhibits cell proliferation and induces apoptosis in CD133 + population in human glioma. Tumour Biol. 2016;37(3):3543–8.
48. Di H, et al. Silencing LDHA inhibits proliferation, induces apoptosis and increases chemosensitivity to temozolomide in glioma cells. Oncol Lett. 2018;15(4):5131–6.
49. Zhang C, et al. RLIP76 Depletion Enhances Autophagic Flux in U251 Cells. Cell Mol Neurobiol. 2017;37(3):555–62.

# Figures

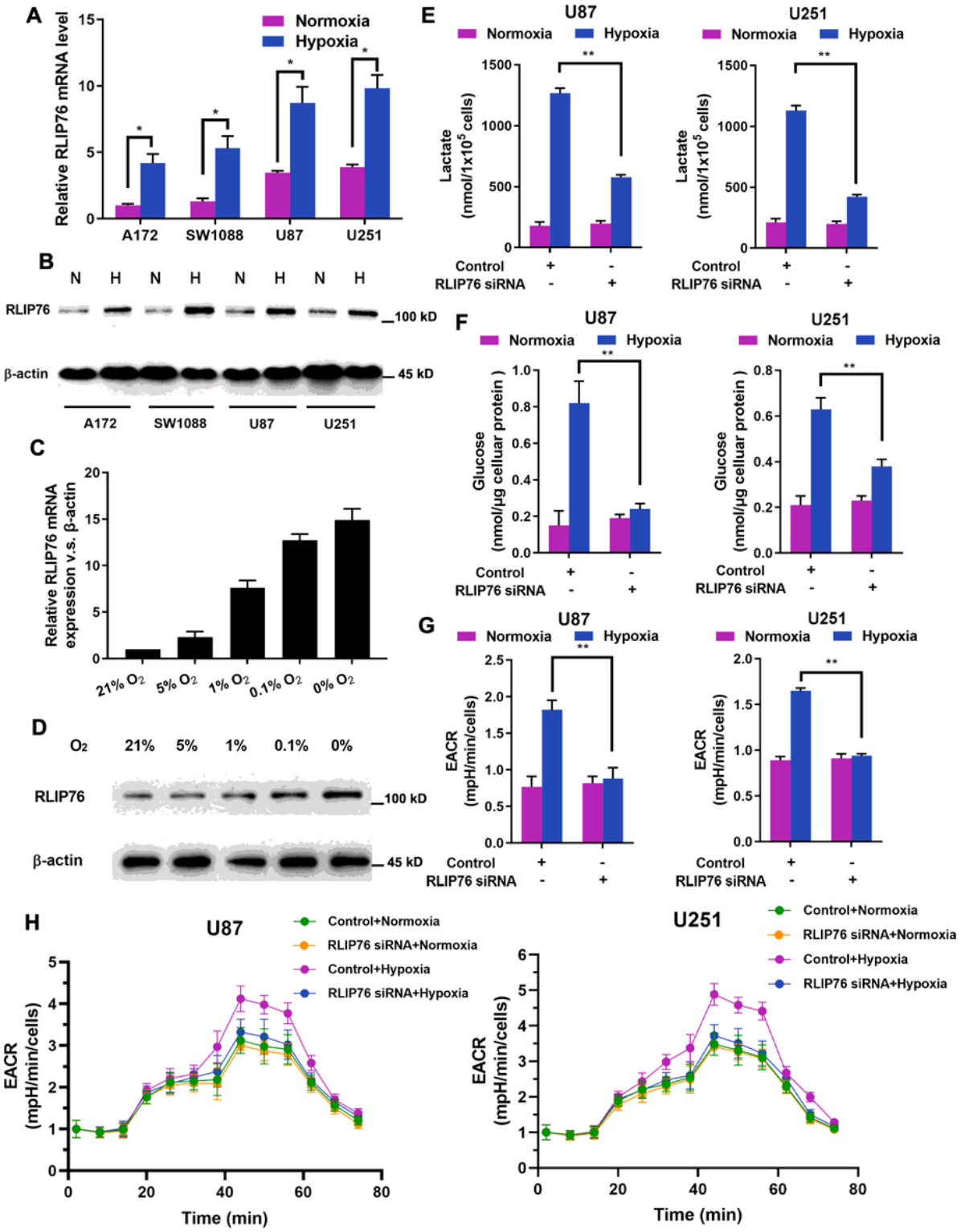


## Figure 1

Hypoxia-Induced RLIP76 Is Required for Hypoxia-Enhanced Glycolysis (A and B) Real-time RT-PCR and Western blotting analysis revealed the RLIP76 mRNA and protein levels in U87, U251, SW1088, and A172 cells with or without hypoxia treatment. All cells were cultured under normoxic (20% O2) or hypoxic (1% O2) conditions for 24 h. Hypoxic conditions (hypoxia) are hereafter defined as the condition of 1% O2 unless otherwise specified. (C and D) U251 cells were cultured under different concentrations of O2 for 24

h. Real-time RT-PCR (C) and Western blotting analysis (D) revealed that RLIP76 expression levels are induced by hypoxia in a dose-dependent manner. (E) U87 and U251 cells transfected with either control or RLIP76 siRNA were cultured under normoxic or hypoxic conditions for 24 h. Levels of lactate in the culture medium were then measured by lactate production assay and normalized to the cell number. **, $P<0.01$. (F) U87 and U251 cells transfected with either control or RLIP76 siRNA were cultured under normoxic or hypoxic conditions for 24 h. Intracellular glucose levels were then measured by glucose uptake assay and normalized according to the protein concentration. **, $P<0.01$. (G) U87 and U251 cells transfected with either control or RLIP76 siRNA were cultured under normoxic or hypoxic conditions for 24 h. Relative glycolytic capacity was measured by the ECAR and normalized to the cell number. **, $P<0.01$. (H) U87 and U251 cells transfected with either control or RLIP76 siRNA were cultured under normoxic or hypoxic conditions for 24 h. The real-time assessment of the ECAR in cultured cells was examined by a Seahorse XFe96 analyzer.

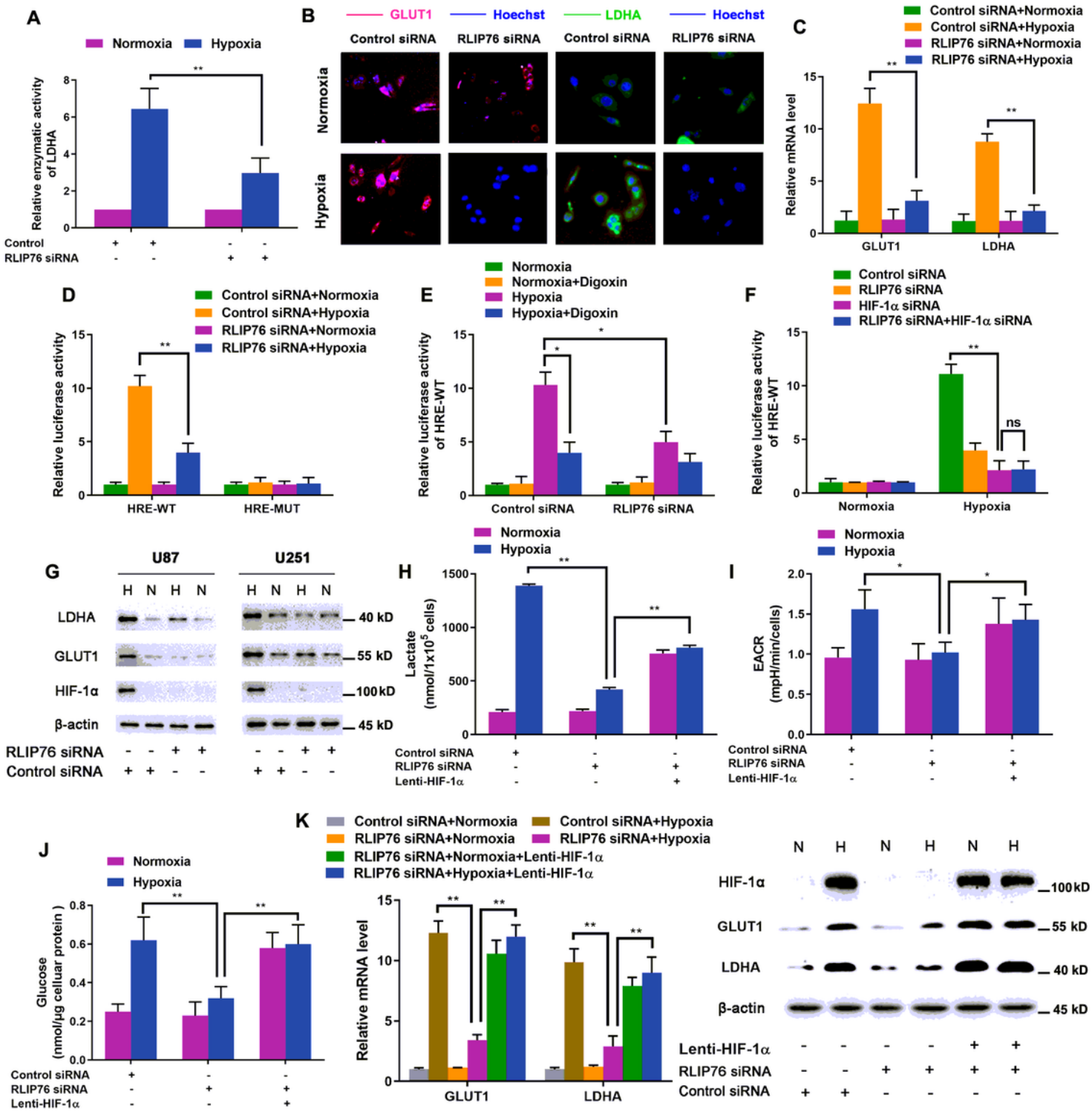


## Figure 2

RLIP76 Regulates Hypoxia-Enhanced Glycolysis via a HIF-1α-Dependent Mechanism (A) U251 cells transfected with either control or RLIP76 siRNA were cultured under normoxic or hypoxic conditions for 24 h. The enzymatic activity of LDHA was normalized to the total protein content. **, P<0.01. (B) U251 cells transfected with either control or RLIP76 siRNA were cultured under normoxic or hypoxic conditions for 24 h. Immunofluorescence analysis was used to examine GLUT1 and LDHA expressions. (C) U251

cells transfected with either control or RLIP76 siRNA were cultured under normoxic or hypoxic conditions for 24 h. Real-time RT-PCR analysis was used to examine GLUT1 and LDHA mRNA levels. **, P<0.01. (D) U251 cells treated with either control or RLIP76 siRNA were cotransfected with the indicated reporter constructs and Renilla luciferase plasmid. Twelve hours after transfection, the cells were cultured under normoxic or hypoxic conditions for 24 h. Reporter activity was calculated by normalization of luciferase activity to Renilla luciferase activity. **, P<0.01. (E) U251 cells treated with either control or RLIP76 siRNA were cotransfected with the indicated reporter constructs and Renilla luciferase plasmid. Twelve hours after the completion of transfection, cells were cultured under normoxic or hypoxic conditions for 24 h. Reporter activity was calculated by normalization of firefly luciferase activity to Renilla luciferase activity. **, P<0.01. The expression levels of HIF-1α are shown in Figure S2A. (F) U251 cells expressing control, RLIP76 siRNA, HIF-1α siRNA, or both RLIP76 siRNA and HIF-1α siRNAs were cotransfected with the HRE reporter construct and Renilla luciferase plasmid. Twelve hours later, cells were cultured under normoxic or hypoxic conditions for 24 h. Reporter activity was calculated by normalization of firefly luciferase activity to Renilla luciferase activity. **, P<0.01. The expression levels of HIF-1α are shown in Figure S2B. (G) U251 and U87 cells transfected with either control or RLIP76 siRNA were cultured under normoxic or hypoxic conditions for 24 h. Western blotting was used to examine HIF-1α, GLUT1 and LDHA expression levels. (H, I and J) U251 cells treated with either control or RLIP76 siRNA were transfected with or without Lenti-HIF-1α. Twenty-four hours after transfection, the cells were cultured under normoxic or hypoxic conditions for 24 h. Lactate levels (H), ECAR values (I) and intracellular glucose levels (J) were then examined. (K) U251 cells treated with either control or RLIP76 siRNA were transfected with or without Lenti-HIF-1α. Twenty-four hours after transfection, the cells were cultured under normoxic or hypoxic conditions for 24 h. Real-time RT-PCR and Western blotting were used to measure LDHA, GLUT1, and HIF-1α mRNA and protein expression levels, respectively.

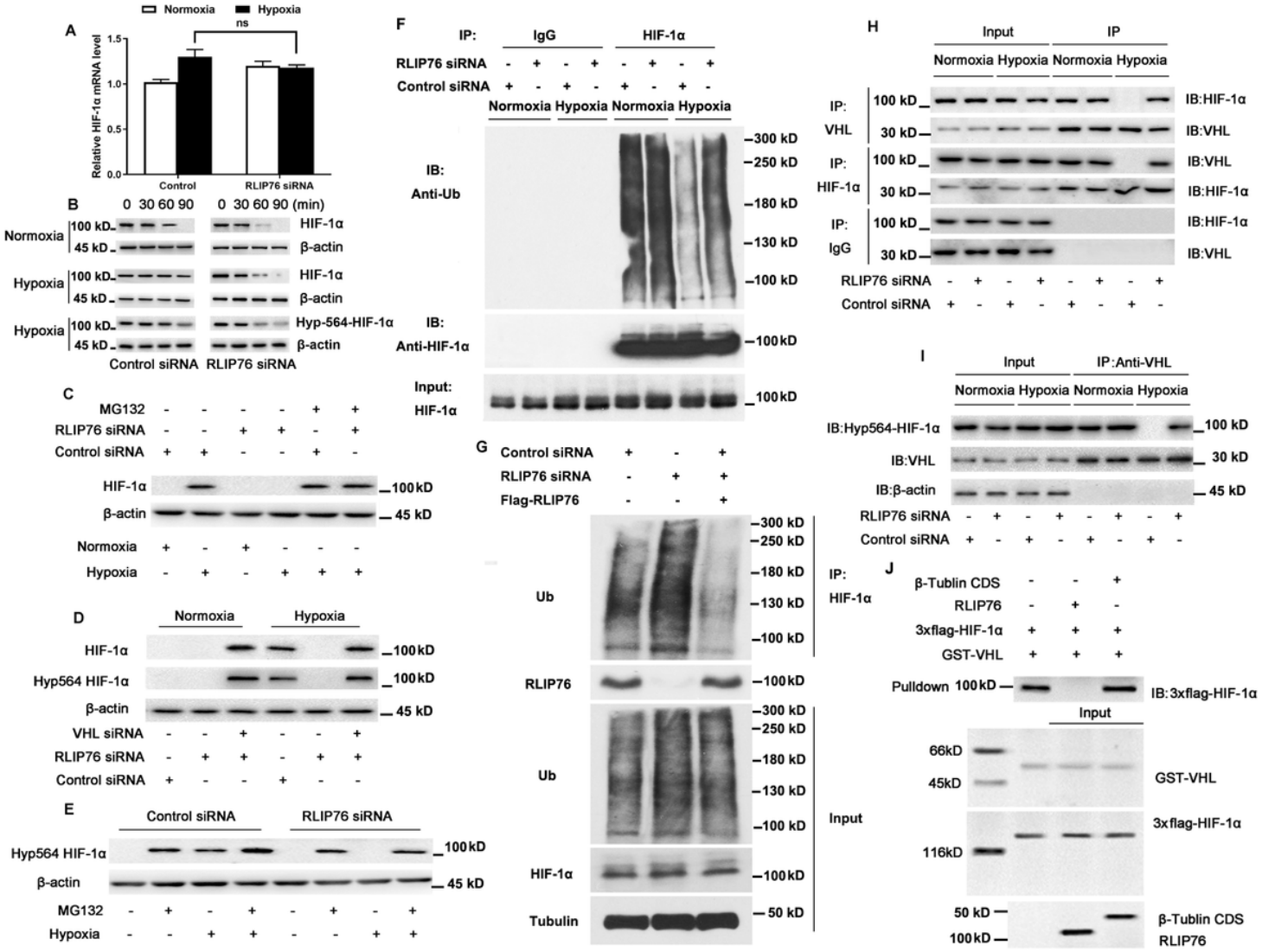


## Figure 3

Hypoxia-Induced RLIP76 Stabilizes HIF-1α (A) U251 cells transfected with either control or RLIP76 siRNA were cultured under normoxic or hypoxic conditions for 24 h. Real-time RT-PCR analysis showed the mRNA expression level of RLIP76. “ns” means no significance. (B) U251 cells were transfected with either control or RLIP76 siRNA. Twelve hours after transfection, the cells were cultured under normoxic or hypoxic conditions. After culturing for 24 h, cycloheximide was used in the indicated cells for the specified periods of time. HIF-1α and hyp564-HIF-1α protein expression levels were determined by Western blotting. (C) U251 cells expressing either control or RLIP76 siRNA were cultured under normoxic or hypoxic conditions with or without 5 μM MG132 treatment for 24 h. HIF-1α protein expression levels were determined by Western blotting. (D) U251 cells transfected with control siRNA, RLIP76 siRNA, or cotransfected with VHL and RLIP76 siRNAs were cultured under normoxic or hypoxic conditions for 24 h. HIF-1α and hyp564-HIF-1α protein expression levels were determined by Western blotting. (E) U251 cells expressing either control or RLIP76 siRNA were cultured under normoxic or hypoxic conditions with or without 5 μM MG132 treatment for 24 h. Hyp564-HIF-1α protein expression levels were determined by Western blotting. (F) Cell lysates were immunoprecipitated with either control IgG or anti-HIF-1α antibody.

The cells were cultured under normoxic or hypoxic conditions in the presence of 5 μM MG132 for 24 h. The immunoprecipitates and input were analyzed by Western blotting. (G) RLIP76 promotes HIF-1α ubiquitination. U251 cells transfected with control siRNA or RLIP76 siRNA together with empty vector or Flag-RLIP76 (Lenti-RLIP76) plasmids were treated with hypoxia in the presence of 5 μM MG132 for 24 h. Cell lysates were denatured and immunoprecipitated with an anti-HIF-1α antibody. Ubiquitination was detected with an anti-ubiquitin antibody. (H) Control IgG, anti-VHL, or anti-HIF-1α antibody was used in immunoprecipitation. The immunoprecipitates and input were analyzed by Western blotting. (I) U251 cells transfected with either control or RLIP76 siRNA were cultured under normoxic or hypoxic conditions in the presence of 5 μM MG132 for 24 h. Cell lysates were immunoprecipitated with anti-VHL antibody. The immunoprecipitates and input were subjected to Western blotting. (J) GST-VHL bound proteins were incubated with purified recombinant flag-HIF-1α in the presence or absence of in vitro transcribed RLIP76 for 3 h. The beads were subjected to Western blotting.

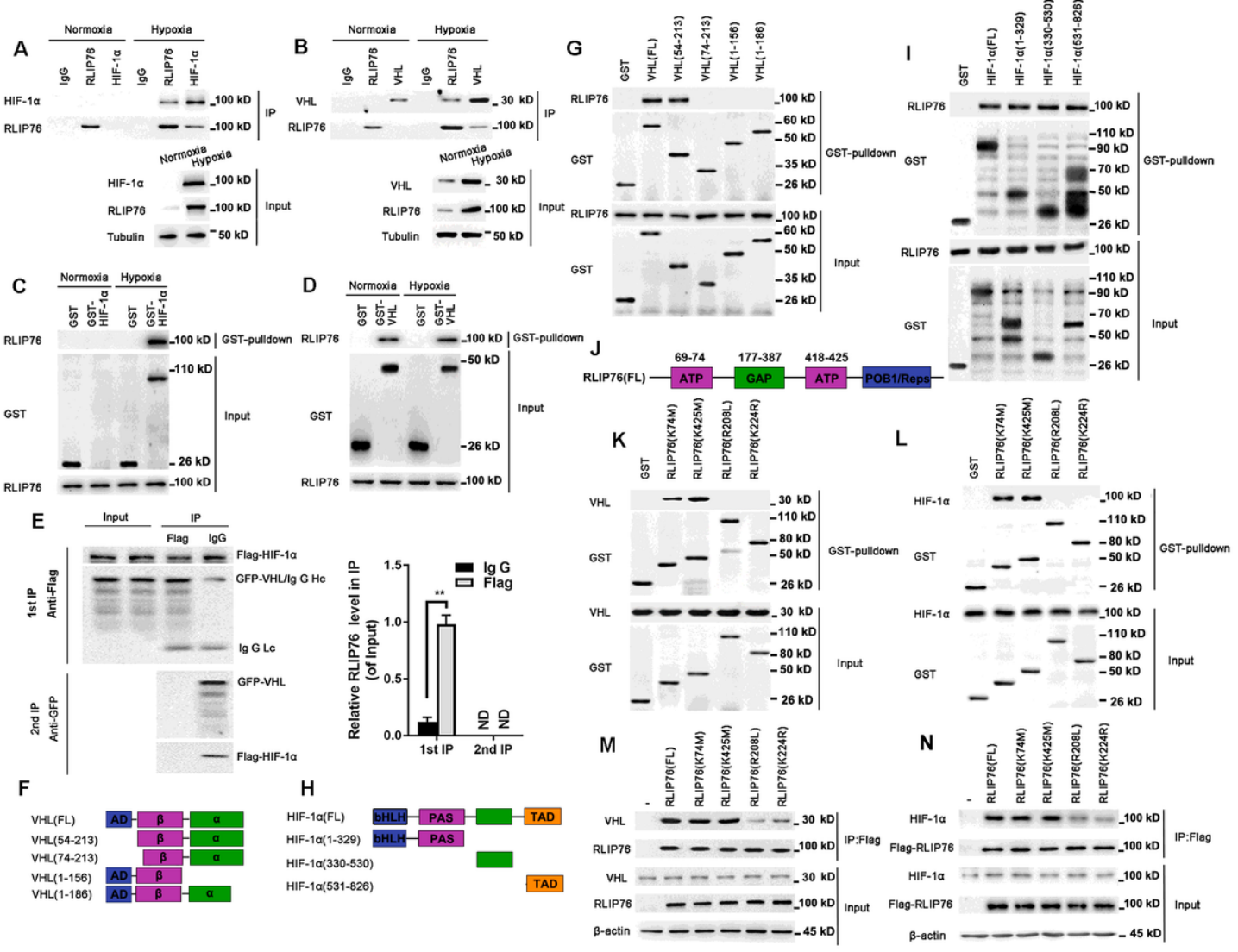


## Figure 4

RLIP76 Interacts with HIF-1α and VHL in a GAP-Dependent Mechanism (A) U251 cells were cultured under hypoxic conditions for 24 h before co-IP assays were conducted. Control IgG and anti-HIF-1α antibody

were used in co-IP assays. **, P<0.01. (B) U251 cells were cultured under hypoxic conditions for 24 h before co-IP assays were conducted. Control IgG and anti-VHL antibodies were used in co-IP assays. **, P<0.01. (C) U251 cells were cultured under normoxic or hypoxic conditions for 24 h before GST pull-down assays were conducted. GST-HIF-1α can readily pull-down RLIP76. (D) U251 cells were cultured under normoxic or hypoxic conditions for 24 h. Protein was purified by GST antibody-conjugated columns and incubated with U251 cell lysates and then repurified through immunoprecipitation and subjected to western blotting. GST-VHL can readily pull-down RLIP76. (E) p3×Flag-HIF-1α and pEGFP-VHL were transfected into U251 cells. Twelve hours after transfection, cells were treated with 5 μM MG132 under hypoxia for another 24 h. Anti-Flag antibody or an isotype-matched control IgG were employed in the first immunoprecipitation. 3× Flag peptides were used to elute the proteins in the immunoprecipitates. Ten percent of the eluent was used for Western blotting, and another 10% was analyzed by real-time RT-PCR. The remaining 80% was immunoprecipitated with either control IgG or anti-GFP antibody, and then the immunoprecipitates were washed. Ten percent of this eluent was subjected to Western blotting, and the remaining 90% was analyzed by real-time RT-PCR. ND indicates that RLIP76 was not detectable in the second immunoprecipitates. **, P<0.01. (F) Schematic representation of full-length VHL and its deletion mutants. (G) U251 cells were transfected with full-length VHL or its deletion mutants. Twelve hours after transfection, cells were cultured under hypoxic conditions for an additional 24 h. The purified GST or GST-tagged VHL fragments were mixed with the cell lysates of U251 cells expressing Flag-RLIP76 and then subjected to GST-pulldown. (H) Schematic representation of full-length HIF-1α and its deletion mutants. (I) U251 cells were transfected with full-length HIF-1α or its deletion mutants. Twelve hours after transfection, cells were cultured under hypoxic conditions for an additional 24 h. The purified GST or GST-tagged HIF-1α fragments were mixed with the cell lysates of U251 cells expressing Flag-RLIP76 and then subjected to GST-pulldown. (J) Schematic representation of full-length RLIP76. (K) U251 cells were transfected with full-length RLIP76 or its GAP-deficient or ATP-deficient mutants. VHL in the GST pulldown assay was analyzed by western blotting. (L) U251 cells were transfected with full-length RLIP76 or its GAP-deficient/ATP-deficient mutants. HIF-1α in the GST pulldown assay was analyzed by western blotting. (M) U251 cells were transfected with Flag-full-length RLIP76 or its GAP-deficient/ATP-deficient mutants. Twelve hours after transfection, cells were cultured under hypoxia for an additional 24 h. An anti-Flag antibody or an isotype-matched IgG was used to immunoprecipitate with the cell lysates. VHL in the immunoprecipitates was analyzed by western blotting. (N) U251 cells were transfected with Flag-full-length RLIP76 or its GAP-deficient/ATP-deficient mutants. Twelve hours after transfection, cells were cultured under hypoxia for an additional 24 h. An anti-Flag antibody or an isotype-matched IgG was used to immunoprecipitate with the cell lysates. HIF-1α in the immunoprecipitates was analyzed by western blotting.

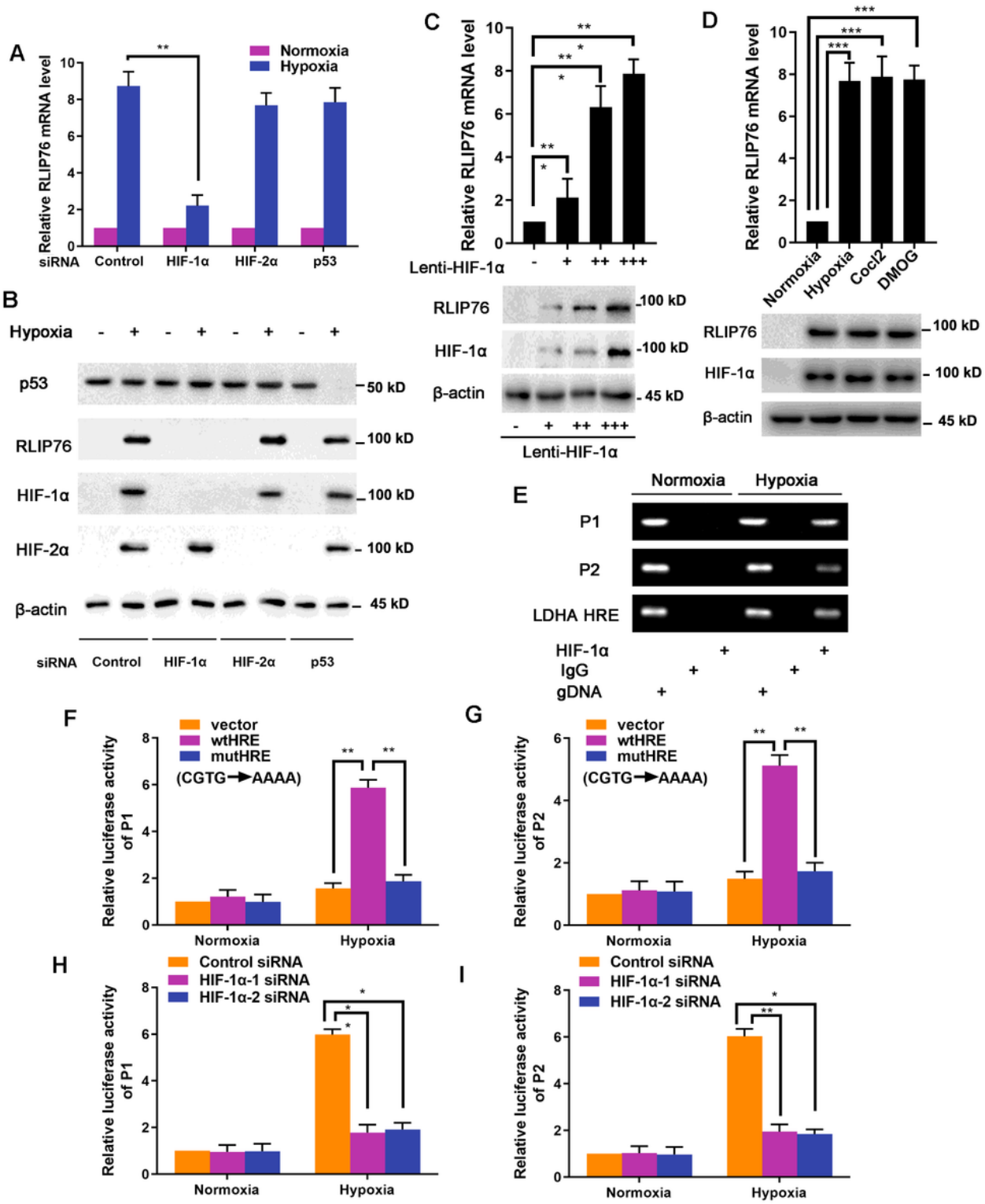


## Figure 5

RLIP76 Is a Direct Target of HIF-1α (A) mRNA levels of RLIP76 measured by quantitative real-time PCR in U251 cells transfected with control siRNA, HIF-1α siRNA, HIF-2α siRNA, or p53 siRNA after culture under normoxic or hypoxic conditions for 24 h. (B) Protein levels of RLIP76 evaluated by Western blotting in U251 cells transfected with control siRNA, HIF-1α siRNA, HIF-2α siRNA, or p53 siRNA after culture under normoxic or hypoxic conditions for 24 h. (C) U251 cells were treated with 0.1 mg, 0.5 mg, or 2 mg Lenti-

HIF-1α. Western blot and real-time RT-PCR analyses were used to measure the protein and mRNA expression levels of RLIP76. **, P<0.01. (D) U251 cells were treated with hypoxia, $CoCl_2$ (100 mM), or DMOG (100 mM). Western blot and real-time RT-PCR analyses were used to measure the protein and mRNA expression levels of RLIP76. ***, P<0.001. (E) Before being subjected to ChIP assay, U251 cells were cultured under normoxic or hypoxic conditions for 24 h. PCR was used to amplify ChIP products. (F and G) The indicated reporter constructs and Renilla luciferase plasmid were cotransfected into U251 cells. Twenty-four hours later, cells were cultured under normoxic or hypoxic conditions for another 24 h. Reporter activity was calculated by normalization of firefly luciferase activity to Renilla luciferase activity. **, P<0.01. (H and I) U251 cells transfected with control siRNA, HIF-1α siRNA-1, or HIF-1α siRNA-2 were cotreated with the HRE-WT reporter constructs and Renilla luciferase plasmid. Twenty-four hours later, cells were cultured under normoxic or hypoxic conditions for another 24 h. Reporter activity was calculated by normalization of firefly luciferase activity to Renilla luciferase activity. **, P<0.01.

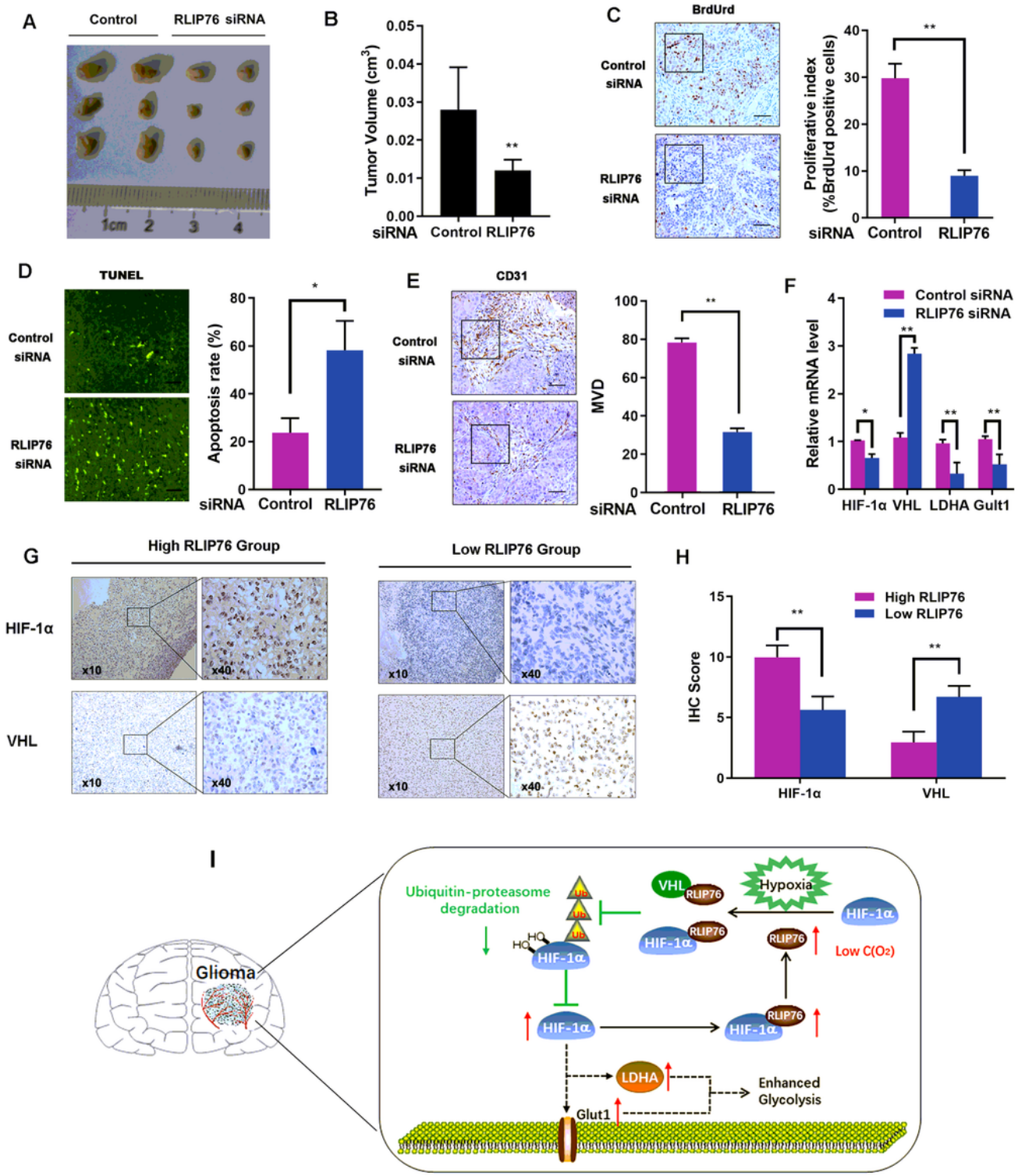


## Figure 6

Hypoxia-Induced RLIP76 is Critical for the Regulation of Tumorigenesis (A and B) Knockdown of RLIP76 suppresses U251 tumor growth in vivo. U251 cells expressing either control siRNA or RLIP76 siRNA were cultured under hypoxic conditions for 36 h and then subcutaneously injected into the flanks of nude mice (n = 6 for each group). (A) Representative images of xenografts were taken 4 weeks after injection. (B) Tumor diameters were measured at the indicated time points, and tumor volumes were calculated.

Significant differences were evaluated by t-test. **, P<0.01. (C) Immunohistochemical analysis of BrdUrd incorporation in subcutaneous tumors originating from the indicated U251 cells. Bar, 20 μm. **, P<0.01. (D) TUNEL staining in subcutaneous tumors originating from the indicated U251 cells. Bar, 20 μm. *, P<0.05. (E) CD31 immunohistochemical staining was carried out in subcutaneous tumors originating from the indicated U251 cell lines. Bar, 20 μm. **, P<0.01. (F) RLIP76, HIF-1α, VHL, LDHA and GLUT1 mRNA expression levels in subcutaneous tumors originating from the indicated U251 cells were measured by quantitative real-time PCR. *, P<0.05; **, P<0.01. (G) Representative images of human GBM specimens immunostained for HIF-1α and VHL. Mean RLIP76: 4.03 ± 0.34; High RLIP76: ≥ 4.03 ± 0.34; High RLIP76: < 4.03 ± 0.34. (H) Quantitative analysis of HIF-1α and VHL staining. **, P<0.01. (I) A diagram showing the potential mechanism of the positive feedback loop between HIF-1α and RLIP76 that promotes glycolysis in hypoxia.

## Supplementary Files

This is a list of supplementary files associated with this preprint. Click to download.

- FigureS3.tif
- FigureS3.tif
- FigureS2.tif
- FigureS2.tif
- FigureS1.tif
- FigureS1.tif
- TableS1.docx
- TableS1.docx